Ceramide kinase uses ceramide provided by ceramide transport protein: localization to organelles of eicosanoid synthesis[S]

Nadia F. Lamour,* Robert V. Stahelin,† Dayanjan S. Wijesinghe,* Michael Maceyka,* Elaine Wang,§ Jeremy C. Allegood,§ Alfred H. Merrill, Jr.,§ Wonhwa Cho, and Charles E. Chalfant[1,*,††]**

Department of Biochemistry,* Medical College of Virginia, Virginia Commonwealth University, Richmond, VA 23298; Department of Biochemistry and Molecular Biology,† Indiana University School of Medicine, South Bend, IN 46617; Department of Biology,§ Georgia Institute of Technology, Atlanta, GA 30332; Department of Chemistry,** University of Illinois at Chicago, Chicago, IL 60607-7061; and Research and Development,†† Hunter Holmes McGuire Veterans Administration Medical Center, Richmond, VA 23249

Abstract Ceramide kinase (CERK) is a critical mediator of eicosanoid synthesis, and its product, ceramide-1-phosphate (C1P), is required for the production of prostaglandins in response to several inflammatory agonists. In this study, mass spectrometry analysis disclosed that the main forms of C1P in cells were $C_{16:0}$ C1P and $C_{18:0}$ C1P, suggesting that CERK uses ceramide transported to the *trans*-Golgi apparatus by ceramide transport protein (CERT). To this end, downregulation of *CERT* by RNA interference technology dramatically reduced the levels of newly synthesized C1P (kinase-derived) as well as significantly reduced the total mass levels of C1P in cells. Confocal microscopy, subcellular fractionation, and surface plasmon resonance analysis were used to further localize CERK to the *trans*-Golgi network, placing the generation of C1P in the proper intracellular location for the recruitment of cytosolic phospholipase $A_2\alpha$. In conclusion, these results demonstrate that CERK localizes to areas of eicosanoid synthesis and uses a ceramide "pool" transported in an active manner via CERT.—Lamour, N. F., R. V. Stahelin, D. S. Wijesinghe, M. Maceyka, E. Wang, J. C. Allegood, A. H. Merrill, Jr., W. Cho, and C. E. Chalfant. **Ceramide kinase uses ceramide provided by ceramide transport protein: localization to organelles of eicosanoid synthesis. *J. Lipid Res.* 2007.** 48: **1293–1304.**

Supplementary key words ceramide-1-phosphate • prostaglandins • phospholipase A_2 • inflammation • arachidonic acid

Ceramide-1-phosphate (C1P) was originally discovered in HL-60 human leukemia cells and synaptic vesicles more than a decade ago (1, 2). In mammalian cells, C1P is produced by the phosphorylation of ceramide by ceramide kinase (CERK) and was first described as a lipid kinase found in brain synaptic vesicles (3, 4). CERK activity was also found to be linked with the membrane fraction and to phosphorylate ceramide but not sphingosine or diacylgycerol (3, 5). Since then, CERK activity has been found in human neutrophils (6, 7), cerebellar granule cells (8), and epithelium-derived A549 lung carcinoma cells (9). Based on its sequence homology to sphingosine kinase type 1, human CERK was cloned recently (5). The cDNA encodes a protein of 537 amino acids with a catalytic domain similar to that of diacylglycerol kinase. Human CERK has an N-terminal pleckstrin homology (PH/PX) domain, which is essential for the activity and the localization of the enzyme at the membrane (5, 10). The enzyme also contains a Ca^+/calmodulin domain at the C terminus (5, 11), which acts as a calcium sensor for the enzyme. Overall, very little is known about the regulation of CERK in cells.

During the last 17 years, several biological effects have been described for C1P. Gomez-Munoz and coworkers (12) showed that C1P was a stimulator of DNA synthesis and promotes cell division. C1P was also shown by the same group to block apoptosis through the inhibition of acid sphingomyelinase in macrophages (13). Other groups have shown that C1P is a mediator of phagocytosis by promoting phagosome formation (14), and two recent reports demonstrated that CERK and C1P are required for activation of the degranulation process in mast cells (11, 15).

Our laboratory was the first to demonstrate that CERK and C1P have distinct roles in eicosanoid synthesis. We

Manuscript received 15 February 2007 and in revised form 23 March 2007.
Published, JLR Papers in Press, March 27, 2007.
DOI 10.1194/jlr.M700083-JLR200

Abbreviations: AA, arachidonic acid; C1P, ceramide-1-phosphate; CERK, ceramide kinase; CERT, ceramide transport protein; $cPLA_2$, cytosolic phospholipase A_2; COX, cyclooxygenase; EEA1, early endosome; EIA, enzyme immuno assay; IL, interleukin; PGE_2, prostaglandin E_2; siRNA, small interfering RNA; TGN, *trans*-Golgi network; TOM20, translocon of the outer membrane; SPR, surface plasmon resonance.

[1] To whom correspondence should be addressed.
e-mail: cechalfant@vcu.edu

[S] The online version of this article (available at http://www.jlr.org) contains supplementary data in the form of four figures.

showed that treatment of several cell types with nanomolar concentrations of C1P induced arachidonic acid (AA) release and the synthesis of eicosanoids (9). Furthermore, studies using pulse labeling demonstrated that the increase in C1P is concurrent with the release of AA and eicosanoids in response to inflammatory agonists (16). Small interfering RNA (siRNA) technology to downregulate CERK blocked cytosolic phospholipase $A_2\alpha$ ($cPLA_2\alpha$) activation, AA release, and eicosanoid production in response to inflammatory cytokines, ATP, and the calcium ionophore A23187 (9). Lastly, our laboratory defined the first intracellular target of C1P, $cPLA_2\alpha$, demonstrating that C1P interacted directly with the enzyme and functioned to increase the association of $cPLA_2\alpha$ with membranes (16). These data demonstrated a new role for CERK and its product, C1P, as major regulators of eicosanoid synthesis via the direct activation of $cPLA_2\alpha$ (16).

In this study, we show that C1P subspecies are enriched in $C_{16:0}$ C1P and $C_{18:0}$ C1P in cells, and we also demonstrate that CERK requires ceramide transported in an active manner by ceramide transport protein (CERT). Moreover, we examined the localization of CERK, and the results disclosed that CERK localizes to the *trans*-Golgi network (TGN), in accordance with the cellular compartment that $cPLA_2\alpha$ translocates when activated by inflammatory agonists (e.g., A23187 and ATP) (17).

EXPERIMENTAL PROCEDURES

Cell culture

All cultured cells were obtained from the American Type Culture Collection. A549 lung adenocarcinoma cells were grown in 50% DMEM (BioWhittaker) and 50% RPMI (BioWhittaker) supplemented with 10% fetal bovine serum (Invitrogen) and 2% penicillin/streptomycin (BioWhittaker). Cells were maintained under 5% CO_2 at 37°C by routine passage every 3 days. HeLa cells were grown in DMEM supplemented with 10% fetal bovine serum and 2% penicillin/streptomycin under the same conditions. For treatments, the medium was replaced 2 h before the addition of the agonist by DMEM containing 2% fetal bovine serum and 2% penicillin/streptomycin.

RNA interference

Sequence-specific silencing of CERK and CERT was performed using sequence-specific siRNA purchased from Dharmacon as described previously (18). The human CERK RNA interference sequence starts at 142 nucleotides from the start codon (UGCCUGCUCUGUGCCUGUAdTdT and UACAGGCACAGAGCAGGCAdTdT) (9). The siRNA for human CERT was from Dharmacon (catalog No. M-012101-00). The sequence targets accession numbers NM_005713 and NM_031361. They were transfected into A549 cells using Dharmafect (Dharmacon) according to the manufacturer's instructions. After incubation for 24, 48, or 72 h, cells were analyzed by Western blotting using a specific antibody against CERK or CERT. After incubation for 48 h, cells were analyzed for C1P levels by TLC or mass spectrometry.

Immunoblotting

Western blot analysis was performed as described previously (19, 20) using 10 μg of protein from each extract. Rabbit anti-CERK (1:1,000), rabbit anti-6XHis (1:1,000) (Sigma), rabbit anti-CERT (1:100) (a gracious gift from Dr. J. Saus and F. Revert-Ros) (21, 22), and mouse anti-CERK (1:10) were used to identify proteins of interest.

C1P analysis

Pulse labeling. A549 cells were plated on 10 cm dishes at the concentration of 1×10^6 per plate. The next day, the cells were transfected with control (scrambled) or CERT siRNA. After a 48 h incubation, [^{32}P]orthophosphate (Perkin-Elmer) was added at 30 μCi/ml for 4 h. The plates were then placed on ice, and the lipids were extracted using the Bligh and Dyer method (23) followed by a base hydrolysis with 0.4 M methanolic NaOH for 2 h at 37°C (24). The samples were dried under N_2 and stored at −80°C. For detection of C1P, the samples were resuspended in chloroform-methanol (75:25) and spotted onto a 10 × 10 cm TLC plate (silica gel) (VWR International). The lipids were separated using a chloroform-acetone-methanol-acetic acid-water (10:4:3:2:1) solvent mixture. The ^{32}P-labeled lipids were detected by exposing the plates to X-ray film.

Mass spectrometric analysis. A549 cells were plated on 10 cm plates in the appropriate medium and grown at 37°C under 5% CO_2 overnight. The next day, cells were treated with ATP (0.1 mM) for 30 min, A23187 (1 μM) for 10 min, or siRNA for 48 h. After treatment, the cells were washed in cold PBS and harvested in PBS. The cells were pelleted by centrifugation at 2,000 *g* for 10 min. The supernatant was removed, and cell pellets were stored at −80°C until extraction and mass spectrometry analysis. An aliquot of cells was taken for standardization (total DNA). To the rest, internal standards (Avanti) were added (0.5 nmol of C12-sphingomyelin, C12-ceramide, C12-glucosylceramide, and C12-lactosylceramide, 0.5 nmol of C17-sphingosine, C17-sphinganine, C17-sphingosine 1-P, and C17-sphinganine-P, and 0.5 nmol of C12-ceramide-P), lipids were extracted, and C1P was quantified by lipid chromatography electrospray ionization tandem mass spectrometry (25). The mass spectrometry instrument used was a 4000 Q-Trap (Applied Biosystems). Multiple reaction monitoring was carried out using *m/z* 644.6 (molecular ion) and *m/z* 78.9 (PO_3^{-2} ion) for C_{12} C1P. The chromatography apparatus for C1P was a 5 cm × 2.1 mm Discovery C18 5 mm HPLC column. The mobile phase was 60% 58:41:1 CH_3OH/water/HCOOH and 40% 99:1 CH_3OH/HCOOH and 5 mM ammonium formate (26).

Surface plasmon resonance analysis. The kinetics of vesicle-protein binding was determined by surface plasmon resonance (SPR) analysis using a BIAcore X biosensor system (Biacore AB) and the L1 chip as described previously (27, 28). The first flow cell was used as a control cell and was coated with 4,800 resonance units of POPC. The second flow cell contained the surface coated with vesicles with varying lipid membrane mimetic compositions (see Table 3 below) at 4,800 resonance units. After lipid coating, 10 μl of 50 mM NaOH was injected at 100 μl/min three times to remove the loosely bound lipids. Typically, no further decrease in SPR signal was observed after one wash cycle. After coating, the drift in signal was allowed to stabilize at <0.3 resonance units/min before any binding measurements, which were performed at 25°C and a flow rate of 30 μl/min. Ninety microliters of protein sample was injected for an association time of 3 min, and the dissociation was then monitored for 10 min in running buffer. After each measurement, the lipid surface was typically regenerated with a 10 μl pulse of 50 mM NaOH. The regeneration solution was passed over the immobilized vesicle surface until the SPR signal reached the initial background value before protein injection. For data acquisition, five or more

different concentrations [typically within a 10-fold range above and below the equilibrium dissociation constant (K_d)] of the enzyme were used, and data sets were repeated three or more times. When needed, the entire lipid surface was removed with a 5 min injection of 40 mM CHAPS followed by a 5 min injection of 40 mM octyl glucoside at 5 μl/min, and the sensor chip was recoated for the next set of measurements. All data were analyzed using BIAevaluation 3.0 software (Biacore) to determine the rate constants of association (k_a) and dissociation (k_d) as described previously (29–31). The K_d was calculated from rate constants using the equation $K_d = k_d/k_a$.

Confocal microscopy

For confocal microscopy, the cells were seeded onto 22 × 22 mm coverslips (Fisher) on 35 mm diameter plates in their appropriate medium and incubated at 37°C under 5% CO_2 overnight. The next day, cells were transfected with pcDNA (Invitrogen) as a control or pcDNA-CERK using Effectene (Qiagen) according to the manufacturer's instructions. Cells were washed twice with PBS to remove the excess protein and then fixed on the coverslips with 100% cold methanol for 10 min at −20°C. The slides were washed extensively after fixing with PBS containing 10 mM glycine and 0.2% sodium azide. Transfected or wild-type cells were then incubated for 40 min with the first antibody: rabbit anti-6XHis (1:100) (Sigma), rabbit anti-GPP130 (1:100) (Covance), mouse anti-CERK (1:1) (Exalpha), rabbit anti-early endosome (EEA1; 1:100) (Abcam), rabbit anti-translocon of the outer membrane (TOM20; 1:100) (a gracious gift from Dr. B. Wattenberg), rabbit anti-TGN46 (1:100) (Abcam), rabbit anti-calreticulin (1:100) (Stressgen), rabbit anti-rab7 (1:100) (Sigma), rabbit anti-cytoC (1:100) (AnaSpec, Inc.), rabbit anti-cyclooxygenase (COX)-2 (1:100) (Cayman), or goat anti-cPLA$_2\alpha$ (1:100) (Santa Cruz Biotechnology). After washing with PBS, FITC, or Cy5-conjugated anti-rabbit antibody (1:200) (Jackson ImmunoResearch), Texas Red-conjugated anti-mouse antibody (1:200) (Jackson ImmunoResearch) and/or FITC-conjugated anti-goat antibody (Jackson ImmunoResearch) was added as appropriate and incubated for 40 min at room temperature. Coverslips were mounted in 10 mM *n*-propagalate in glycerol and viewed using a Leica confocal microscope. Quantification of colocalization was accomplished as described (32) using Zeiss LSM510 software.

Prostaglandin E_2 assay

The ELISA plate (Cayman Chemical), coated with goat anti-mouse IgG, was loaded at 50 μl per well of standard per sample, where the sample was diluted 1:40 in 1× enzyme immuno assay (EIA) buffer, 50 μl of prostaglandin E_2 (PGE_2) EIA acetylcholinesterase tracer (Cayman Chemical), and 50 μl of PGE_2 monoclonal antibody (Cayman Chemical). The control wells received 50 μl of 1× EIA buffer along with 50 μl of PGE_2 EIA acetylcholinesterase tracer and 50 μl of PGE_2 monoclonal antibody. The plate was covered and kept at 4°C for 16 h. The plate was then washed, and 200 μl of Ellman's reagent (Cayman Chemical) was added to each well and allowed to develop in the dark with low shaking at room temperature for 90 min. After the developing step, absorbance in each well at 405 nM was read using a microplate spectrophotometer (BMG Labtech FLUOStar Optima). This assay was normalized by WST-1 assay (Roche Diagnostics) according to the manufacturer's instructions. WST-1 reagent (10% of the total volume) was added to the cells, and the plate was incubated at 37°C for 30 min. The optical density was then measured (at 450 nM vs. a reference of 630 nM) using a microplate spectrophotometer (BIO-TEK KC Junior).

Adenovirus transfection

A549 cells were seeded onto 22 × 22 mm coverslips (Fisher) on 35 mm diameter plates in the appropriate medium and incubated at 37°C under 5% CO_2 overnight. The next day, cells were transfected with adenovirus containing 6XHis-CERK and/or green fluorescent protein-cPLA$_2$ at 150 and 40 multiplicity of infection, respectively. After 48 h of incubation, the cells were treated with 1 μM A23187 for 10 min. Cells were washed twice with PBS to remove the excess protein and then fixed on the coverslips with 100% cold methanol for 10 min at −20°C. The slides were washed extensively after fixing with PBS containing 10 mM glycine and 0.2% sodium azide. The cells were then incubated for 40 min with the first antibody, a rabbit anti-6XHis (1:100) (Sigma), and washed with PBS-glycine for a few seconds. Texas-red-conjugated anti-rabbit antibody (1:200) (Jackson ImmunoResearch) was then added and incubated for 40 min at room temperature. Coverslips were mounted in 10 mM *n*-propagalate in glycerol and viewed using a Leica confocal microscope.

Subcellular fractionation

A549 cells (~2 × 10^6) were suspended in buffer containing 20 mM HEPES (pH 7.4), 10 mM KCl, 2 mM $MgCl_2$, 1 mM EDTA, 0.25 M sucrose, and protease inhibitor cocktail (Sigma). Cells were then disrupted by 20 strokes of a Dounce homogenizer. Subcellular fractionation was performed by differential centrifugation as described (33). The postnuclear supernatants were centrifuged at 5,000 *g* for 10 min to generate the heavy membrane (mitochondria- and *trans*-Golgi-enriched fraction). The supernatants were then centrifuged at 17,000 *g* for 15 min to obtain the light membrane fraction (endoplasmic reticulum- and *cis*-Golgi-enriched fraction). Alternatively, postnuclear supernatants were centrifuged directly at 17,000 *g* for 15 min to obtain a fraction containing mitochondria, endoplasmic reticulum, and Golgi. The remaining supernatants were centrifuged at 100,000 *g* for 1 h to obtain the plasma membrane and the cytosol. Ten micrograms of the different fractions was loaded onto a SDS-PAGE gel and analyzed by Western blot using rabbit anti-human mitochondrial antibody (1:1,000) (US Biological), mouse anti-PDI antibody (1:1,000) (Stressgen), rabbit anti-TGN46 antibody (1:1,000) (Abcam), mouse anti-TGN38 antibody (1:1,000) (Affinity Bioreagents), mouse anti-CERK antibody (1:10), rabbit anti-EEA1 antibody (1:500) (Abcam), and rabbit anti-Rab7 antibody (1:500) (Sigma).

RESULTS

C1P is enriched in $C_{16:0}$, $C_{18:0}$, and $C_{20:0}$ subspecies compared with ceramide in cells

Previously, our laboratory demonstrated that CERK phosphorylated a wide spectrum of naturally occurring ceramides irrespective of acyl chain length in vitro (34). Although CERK used a wide spectrum of these ceramide subspecies in vitro with the same catalytic efficiency, analysis of several cell lines, such as A549 cells (**Fig. 1**), HeLa cells, and J774.1 macrophages (see supplementary Fig. I), by mass spectrometry disclosed that the major form of C1P was $C_{16:0}$ C1P, followed by $C_{18:0}$ C1P. The C1P subspecies profile could not be explained by simple ceramide metabolism (the substrate for CERK), as the profiles of specific subspecies of C1P were altered significantly compared with those of ceramides. For example, $C_{24:1}$ and $C_{24:0}$ C1Ps accounted for only 18.4% of total C1P levels

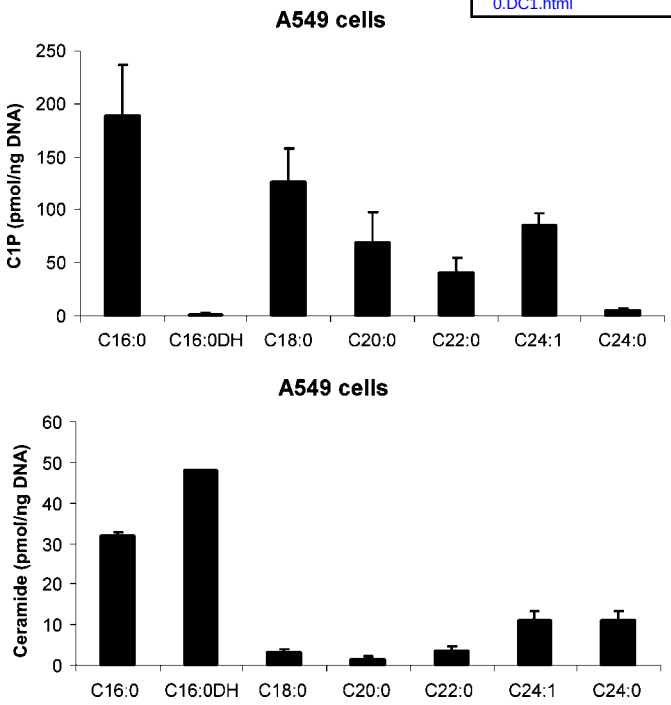

Fig. 1. Ceramide-1-phosphate (C1P) is enriched in $C_{16:0}$, $C_{18:0}$, and $C_{20:0}$ subspecies in cells. Mass spectrometry analysis was used to determine the levels of various species of C1P and ceramide in A549 cells. Data are presented as means of C1P and ceramide (pmol/ng DNA) ± SEM and are representative of four experiments repeated on two separate occasions. C, ceramide; CDH, dihydroceramide.

versus $C_{24:1}$ and $C_{24:0}$ ceramides, which accounted for 34.6% of total ceramides in A549 cells (**Table 1**). Furthermore, the profiles of $C_{18:0}$ and $C_{20:0}$ C1Ps were also significantly different from the profiles of these same ceramides. Whereas $C_{18:0}$ and $C_{20:0}$ C1Ps accounted for 39.5% of the total C1P levels, $C_{18:0}$ and $C_{20:0}$ ceramides accounted for only 7.7% of the total ceramide levels in A549 cells (Table 1). Both of these trends were also observed for the other cell types (see supplementary Fig. I). Another major difference observed between the profiles of ceramide and C1P subspecies was the levels of dihydroceramide compared with dihydro-C1Ps. All cell types produced almost equivalent amounts of $C_{16:0}$ ceramide and $C_{16:0}$ dihydroceramide (Fig. 1; see supplementary Fig. I). In stark contrast, the $C_{16:0}$ dihydro-C1P was almost not detectable.

TABLE 1. C1P and ceramide subspecies profiles

Cell Line	Percentage $C_{18:0}$ + $C_{20:0}$ C1P	Percentage $C_{24:0}$ + $C_{24:1}$ C1P	Percentage $C_{18:0}$ + $C_{20:0}$ Ceramide	Percentage $C_{24:0}$ + $C_{24:1}$ Ceramide
J774.1	35.9	16.9	3.5	34.0
HeLa	40.3	19.95	5.3	32.3
A549	39.5	18.4	7.7	34.6
Raw	9.6	20.4	3.1	59.9

C1P, ceramide-1-phosphate. Mass spectrometry analysis was used to determine the levels of various species of C1P and ceramide in A549, HeLa, J774.1, and Raw cells. This table depicts the percentage of $C_{18:0}$ and $C_{20:0}$ C1P and ceramide among the total mass of C1P and ceramide in cells. (The dihydro subspecies of C1P and ceramide were not included in the calculation.) The same calculation was done for $C_{24:0}$ and $C_{24:1}$. Data are representative of four experiments repeated on two separate occasions.

Our laboratory has shown previously that the well-established activators of AA release and prostanoid synthesis, A23187 and ATP, require CERK for this signaling function. To determine whether the C1P subspecies profile changed in response to inflammatory agonists, A549 cells were treated with ATP and A23187. The major form of C1P, D-e-$C_{16:0}$ C1P, increased significantly in response to these inflammatory agonists. Indeed, $C_{16:0}$ C1P was increased without significant effects on total ceramide levels (**Fig. 2A**). Other chain lengths of C1P were also increased to a similar extent as that of D-e-$C_{16:0}$ C1P (Fig. 2B), but the total mass increase in D-e-$C_{16:0}$ C1P was significantly greater. These data suggest that the subspecies of C1P are formed depending on the substrate availability for CERK, which is preferentially $C_{16:0}$ and $C_{18:0}$ ceramide.

CERT supplies the substrate for CERK in cells

Hanada and coworkers (21, 35) demonstrated that CERT preferentially transported saturated ceramides of ⩽22 carbons (e.g., D-e-$C_{16:0}$, D-e-$C_{18:0}$, and D-e-$C_{20:0}$) from the endoplasmic reticulum to the TGN, also the site of the translocation of the direct target of C1P, cPLA$_2\alpha$. Therefore, we hypothesized that CERT preferentially transported these ceramide subspecies for use by CERK, explaining the enrichment of C1P subspecies in $C_{18:0}$ versus $C_{24:0}$ and $C_{24:1}$. [Of note, CERT will transport longer chain ceramides and those with unsaturated chain lengths, but to a lesser extent than $C_{16:0}$, $C_{18:0}$, and $C_{20:0}$ ceramides (21). CERT also does not efficiently transport dihydroceramide to the *trans*-Golgi (21).] To test our hypothesis, we examined whether CERK used ceramides provided by CERT. Downregulation of CERT (81%) by siRNA interference technology (**Fig. 3A**) induced a dramatic decrease (>80%) in newly synthesized/kinase-derived C1P as measured by pulse labeling with [^{32}P]inorganic phosphate (Fig. 3B). Examining the total mass of C1P using mass spectrometry confirmed the downregulation of total C1P levels (>40% downregulation) (Fig. 3C). Thus, CERK requires ceramide actively transported to the TGN via CERT, explaining the subspecies pattern for C1P and the low levels of dihydro-C1P in cells.

To confirm a physiological role for CERT in C1P formation, downregulation of CERT by siRNA also significantly inhibited the induction of eicosanoid synthesis in response to interleukin (IL)-1β (**Table 2**). This effect of CERT siRNA could not be explained by altering cellular organelles, as the integrity of the Golgi apparatus was conserved (see supplementary Fig. III).

CERK interacts specifically with a Golgi (internal) membrane mimic in vitro

Because CERK used ceramide transported to the *trans*-Golgi apparatus by CERT, we hypothesized that CERK localized to this subcellular compartment. To first test this

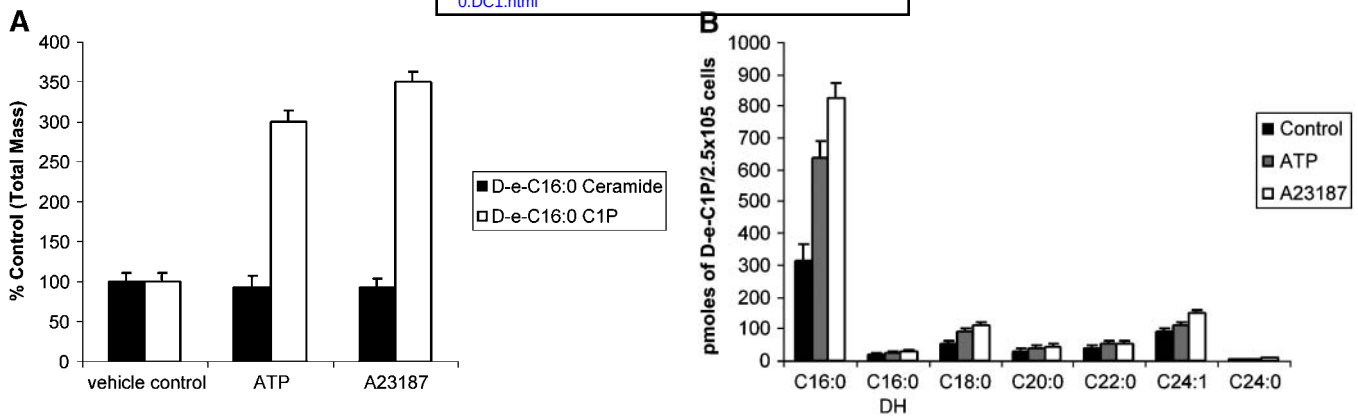

Fig. 2. The inflammatory agonists, ATP and A23197, induce an increase in saturated C1P levels as measured by mass spectrometry. A549 cells were plated on 10 cm diameter plates in appropriate medium and grown at 37°C under 5% CO_2 overnight. The next day, cells were treated with ATP (0.1 mM) for 30 min and A23187 (1 μM) for 10 min. The cells were pelleted and stored at −80°C until extraction and mass spectrometry analysis. A: Levels of C_{16} C1P (white bars) and ceramide (black bars). Data are presented as percentages of control ± SEM and are representative of three different experiments repeated on two separate occasions. B: Data are presented as means of C1P in pmol of D-e-C1P per 2.5×10^5 cells ± SEM (control, black bars; ATP, gray bars; A23187, white bars). CDH, dihydroceramide.

hypothesis, we used SPR to measure the interaction of CERK with immobilized vesicles whose lipid compositions recapitulate those of cellular membranes, specifically the plasma membrane and the Golgi (internal) membrane. Lipid vesicle mimetics have been used extensively to study the targeting behaviors of C2 domains and protein kinase C isoforms (27, 28), and their composition is based upon the reported lipid composition of rat liver cell membranes

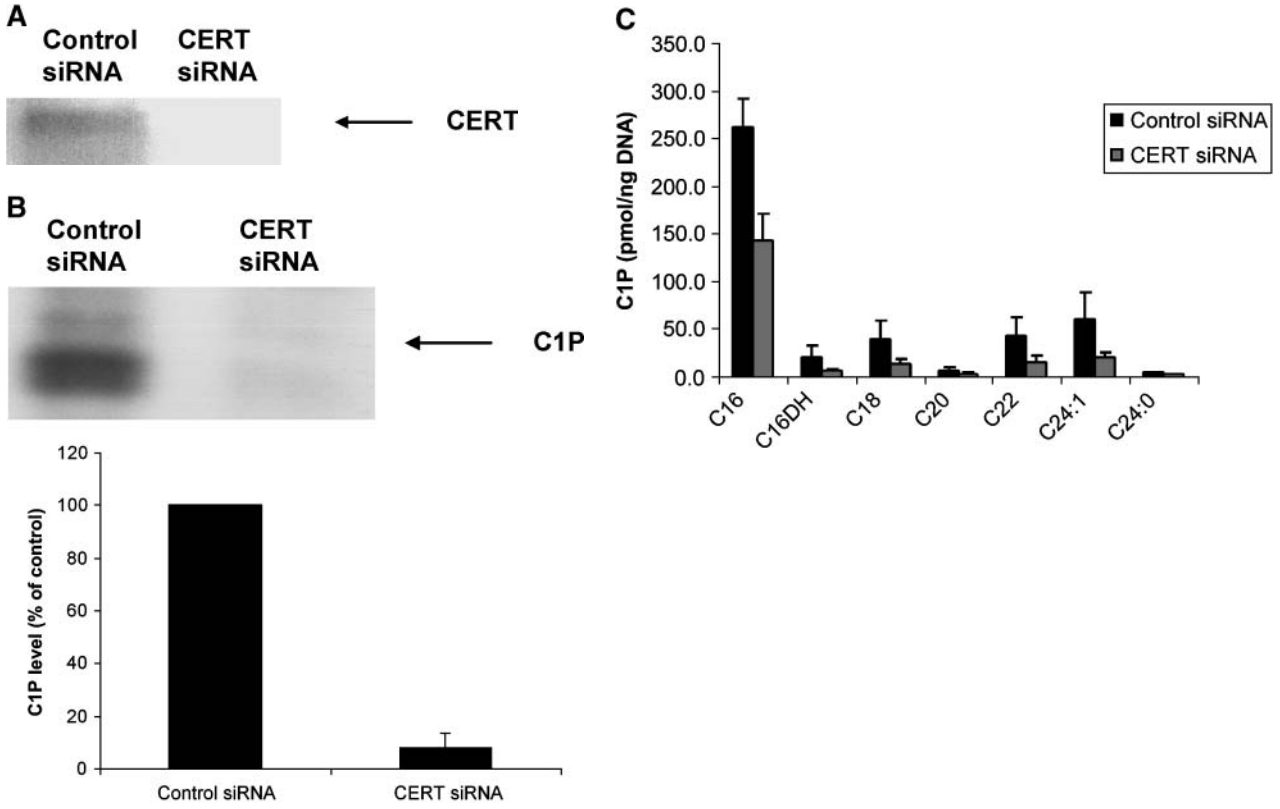

Fig. 3. Ceramide transport protein (CERT) provides the substrate for ceramide kinase (CERK) in cells. Sequence-specific silencing of CERT was performed using small interfering RNA (siRNA) as described in Experimental Procedures. A: Effect of siRNA on CERT expression as measured by Western immunoblot analysis. B: Effect and quantification (percentage of control) of the downregulation of CERT on C1P levels analyzed by pulse labeling with [^{32}P]orthophosphate. C: Effect of the downregulation of CERT on total C1P levels as measured by mass spectrometry (pmol/ng DNA). Data are presented as means of C1P ± SEM ($P < 0.05$, determined by *t*-test) and are representative of four experiments repeated on two separate occasions (control siRNA, black bars; CERT siRNA, gray bars). CDH, dihydroceramide.

TABLE 2. Effect on CERT siRNA on PGE_2 production

siRNA	Treatment	PGE_2
		pg/ml
Control	PBS	14.7 ± 5.1
CERT	PBS	6.6 ± 2.1
Control	IL-1β	368 ± 72
CERT	IL-1β	104 ± 41.9

CERT, ceramide transport protein; IL, interleukin; PGE_2, prostaglandin E_2; siRNA, small interfering RNA. Cells were transfected with siRNA and treated with IL-1β or PBS as described in Experimental Procedures. PGE_2 production was determined by ELISA and normalized using WST-1 assay. Data are presented as means ± SEM ($P < 0.05$, determined by *t*-test) and are representative of two independent experiments (n = 6).

(36). Experiments were performed in 10 mM MOPS, pH 7.2, containing 0.15 M KCl, 2 mM EGTA, 1 mM DTT, and 5% glycerol using a control sensor surface of POPC. POPC was used as a control, as no binding to POPC was observed over the background for CERK concentrations up to 10 μM. In general, CERK showed high affinity (i.e., low nanomolar to subnanomolar K_d) for both membrane mimetics, suggesting that it may be largely membrane-bound at steady state. In particular, CERK showed the highest affinity for the Golgi (internal membrane) mimetic (**Table 3**), consistent with its preferential use of ceramides in the *trans*-Golgi apparatus. In fact, CERK bound with 6-fold greater affinity to the Golgi (internal membrane) mimetic than to the plasma membrane mimetic, mainly attributable to a smaller k_d for the internal membrane mimetic. Increases and decreases in affinity as low as 3-fold have been implicated in altering, abolishing, and/or enhancing the subcellular localization of many peripheral proteins (27, 28). It should be noted that our mimetics may not fully simulate cell membranes and that the Golgi (internal membrane) mimetic has an average lipid composition of *cis*-Golgi network and TGN, which are known to have nonuniform lipid compositions. With these caveats, our results support the notion that CERK is recruited to and localized to internal membranes, possibly the Golgi apparatus. The high affinity of CERK for the plasma membrane mimetic also suggests that CERK may be localized to other cellular membranes under certain conditions and is predominantly membrane-bound in cells.

CERK localizes to the TGN, mitochondria, and endosomes/exosomes

Our laboratory previously found that treatment of cells with C1P induced the "classical" translocation of $cPLA_2\alpha$ from the cytosol to the *trans*-Golgi apparatus (16). Furthermore, we have shown that CERK and C1P are required for this activation. Therefore, based on these data, the use of ceramides transported to the *trans*-Golgi by CERT, and the high affinity of CERK for the Golgi (internal membrane) mimetic, we hypothesized that CERK localizes to the *trans*-Golgi apparatus, the site of $cPLA_2\alpha$ translocation. To investigate this hypothesis, we used a newly developed monoclonal antibody for CERK and examined whether this antibody specifically recognized CERK by Western immunoblotting techniques. The antibody recognized one major protein of ~62 kDa (**Fig. 4A**). This protein was shown to be specifically downregulated by a validated and specific siRNA targeted against human CERK (Fig. 4A) (9).

Second, the ability of the antibody to recognize CERK by immunocytochemistry techniques was also determined. The cDNA for human CERK tagged with a 6XHis epitope was transiently expressed in A549 cells. By Western blot, we examined whether the protein containing the 6XHis tag was expressed. Anti-6XHis antibody recognized a major protein of ~62 kDa (Fig. 4B), the same size as CERK. The cells were double stained with a polyclonal antibody against the 6XHis epitope and the anti-CERK monoclonal antibody. Using confocal microscopy, both antibodies demonstrated that CERK was localized to a perinuclear region indicative of the Golgi apparatus in A549 cells (Fig. 4C) and HeLa cells (data not shown). The nuclear signal with the anti-6XHis was nonspecific and present in the cells not expressing the recombinant CERK (see supplementary Fig. IV). The anti-CERK antibody pattern overlaid the perinuclear pattern of the 6XHis antibody. Thus, the CERK monoclonal antibody specifically recognizes CERK expressed in cells.

To demonstrate the localization of the endogenous CERK, we again used the monoclonal antibody specific to CERK along with antibodies raised against various subcellular markers (**Fig. 5**) for the endoplasmic reticulum (calreticulin) (Fig. 5A), the *cis*-Golgi network (GPP130) (Fig. 5B), the *trans*-Golgi (TGN46) (Fig. 5C), EEA1 (Fig. 5D),

TABLE 3. CERK interacts specifically with a Golgi "internal" membrane mimic determined by SPR analysis

Mimic	k_a	k_d	K_d
	$M^{-1}\ s^{-1}$	s^{-1}	M
Plasma membrane mimetic POPC/POPE/SM/POPS/POPI/cholesterol (12:33:6:20:9:20)	$(4.0 \pm 0.5) \times 10^5$	$(1.8 \pm 0.3) \times 10^{-3}$	$(4.5 \pm 0.9) \times 10^{-9}$
Golgi mimetic POPC/POPE/SM/POPS/POPI/cholesterol (43:17:13:5:10:12)	$(5.5 \pm 0.6) \times 10^5$	$(4.1 \pm 0.5) \times 10^{-4}$	$(7.5 \pm 1.0) \times 10^{-10}$

CERK, ceramide kinase; POPE, palmitoyl oleoyl phosphatidyl ethanolamine; POPS, palmitoyl oleoyl phosphatidyl serine; POPI, palmitoyl oleoyl phosphatidyl inositol; SM, sphingomyelin; SPR, surface plasmon resonance. To better understand the subcellular targeting behavior of CERK, we measured its binding to immobilized vesicles whose lipid compositions recapitulate those of cellular membranes. The kinetics of vesicle-protein binding was determined by SPR analysis using a BIAcore X biosensor system as described in Experimental Procedures to determine the rate constants of association (k_a) and dissociation (k_d). The equilibrium dissociation constant (K_d) was calculated from rate constants using the equation $K_d = k_d/k_a$. The table depicts the K_d of the interaction of CERK with each membrane mimetic. Data are expressed as means ± SEM and are representative of four experiments repeated on two separate occasions.

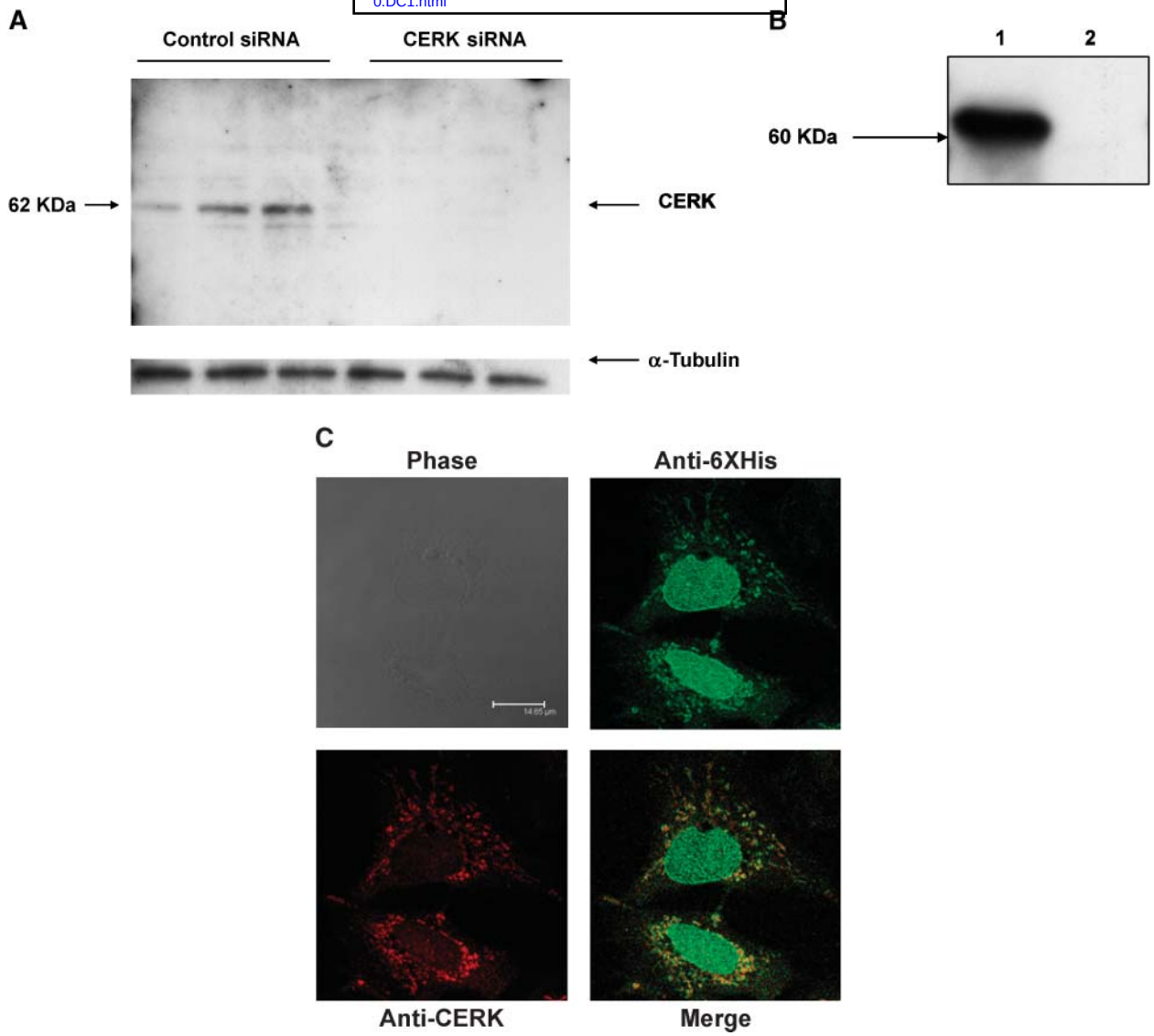

Fig. 4. The anti-CERK antibody specifically recognizes the enzyme. A: A549 cells were transfected as described in Experimental Procedures with either control siRNA (200 nM) or siRNA specific to human ceramide kinase (200 nM) for 48 h. The level of CERK was examined by Western immunoblot using the monoclonal antibody specific to CERK. Data are representative of three different experiments. B: A549 cells were transfected as described in Experimental Procedures with pCDNA-CERK (lane 1) or pCDNA (lane 2). The level of recombinant protein was examined by Western blot using an anti-6XHis antibody. C: For confocal microscopy, the A549 cells were seeded onto coverslips. The next day, cells were transfected with pcDNA-CERK(6XHis) or pcDNA (Invitrogen) vector and then fixed with 100% cold methanol for 10 min at −20°C. The slides were washed extensively after fixing with PBS containing 10 mM glycine and 0.2% sodium azide. The cells were then incubated for 40 min with the primary antibodies, a rabbit anti-6XHis (1:100) (green) and the mouse anti-CERK (1:1) (red). Data are representative of four different experiments.

mitochondria (TOM20) (Fig. 5E), and late endosomes/exosomes (Rab7) (Fig. 5F). Figure 5 demonstrates that CERK does not significantly localize to the endoplasmic reticulum (<40%) or the *cis*-Golgi network (<21%). On the other hand, CERK demonstrated significant colocalization with the *trans*-Golgi marker TGN46 (>50%). Significant colocalization was also observed with markers for EEA1 (60%) and markers for the late endosomal/exosomal compartment, Rab7 (66%). These data demonstrate that CERK preferentially localizes to internal membranes.

Based on these results and the use of ceramides provided by CERT, we hypothesized that CERK localized to the same compartment (*trans*-Golgi) as activated cPLA$_2$α. To investigate this hypothesis, A549 cells were transfected with adenovirus containing the two enzymes, as described in Experimental Procedures. Upon treatment by A23187, **Fig. 6** demonstrated that cPLA$_2$α translocated to the same compartment as CERK. Because activated cPLA$_2$α was localized to the *trans*-Golgi using a TGN46 antibody (37) in cells, our data demonstrate that CERK localizes to the *trans*-Golgi apparatus, in accord with cPLA$_2$α activation by inflammatory agonists.

Interestingly, CERK also demonstrated colocalization with the marker for the outer mitochondrial membrane,

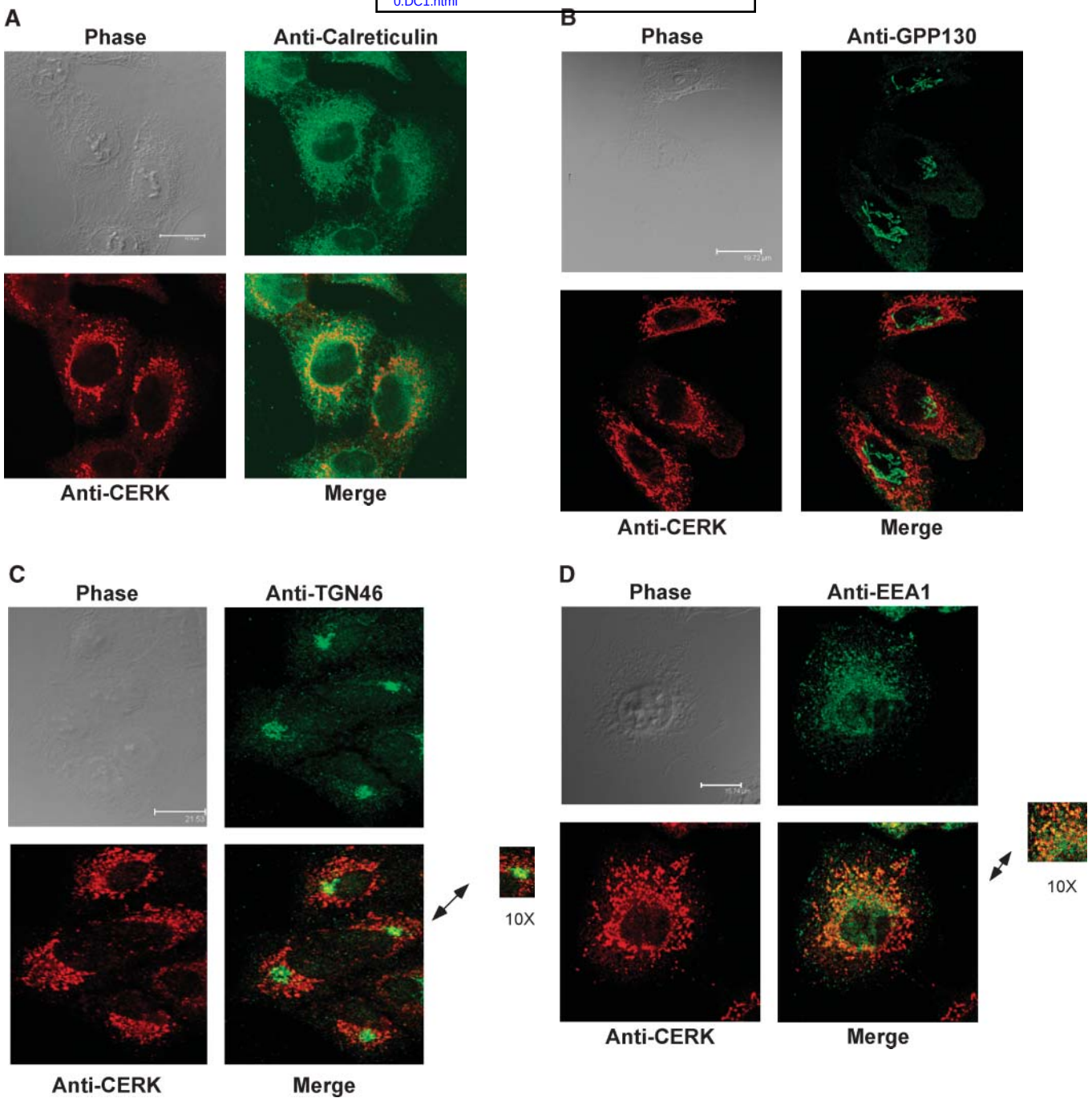

Fig. 5. CERK localizes to the *trans*-Golgi apparatus, mitochondria, and endosomal/exosomal compartments. For confocal microscopy, the cells were seeded onto 22 × 22 mm coverslips on 35 mm diameter plates in appropriate medium and incubated at 37°C under 5% CO_2 overnight. Cells were washed twice with PBS to remove the excess protein and then fixed with 100% cold methanol for 10 min at −20°C. The slides were washed extensively after fixing with PBS containing 10 mM glycine and 0.2% sodium azide. A: Cells were incubated with the primary antibodies, a rabbit anti-calreticulin (1:100) (green) and a mouse anti-CERK (1:1) (red) for 40 min. B: Cells were incubated with the primary antibodies, a rabbit anti-GPP130 (1:100) (green) and a mouse anti-CERK (1:1) (red) for 40 min. C: Cells were incubated with the primary antibodies, a rabbit anti-*trans*-Golgi network (TGN)46 (1:100) (green) and a mouse anti-CERK (1:1) (green) for 40 min. D: Cells were incubated with the primary antibodies, a rabbit anti-early endosome (EEA1; 1:100) (green) and a mouse anti-CERK (1:1) (red) for 40 min. E: Cells were incubated with the primary antibodies, a rabbit anti-translocon of the outer membrane (TOM20; 1:100) (green) and a mouse anti-CERK (1:1) (red) for 40 min. F: Cells were incubated with the primary antibodies, a rabbit anti-Rab7 (1:100) (green) and a mouse anti-CERK (1:1) (red) for 40 min. G: Cells were incubated with the primary antibodies, a rabbit anti-cyclooxygenase (COX)-2 (1:100) (green) and a mouse anti-CERK (1:1) (red) for 40 min. Coverslips were mounted in 10 mM *n*-propagalate in glycerol and were viewed using a Leica confocal microscope. Data are representative of three different experiments.

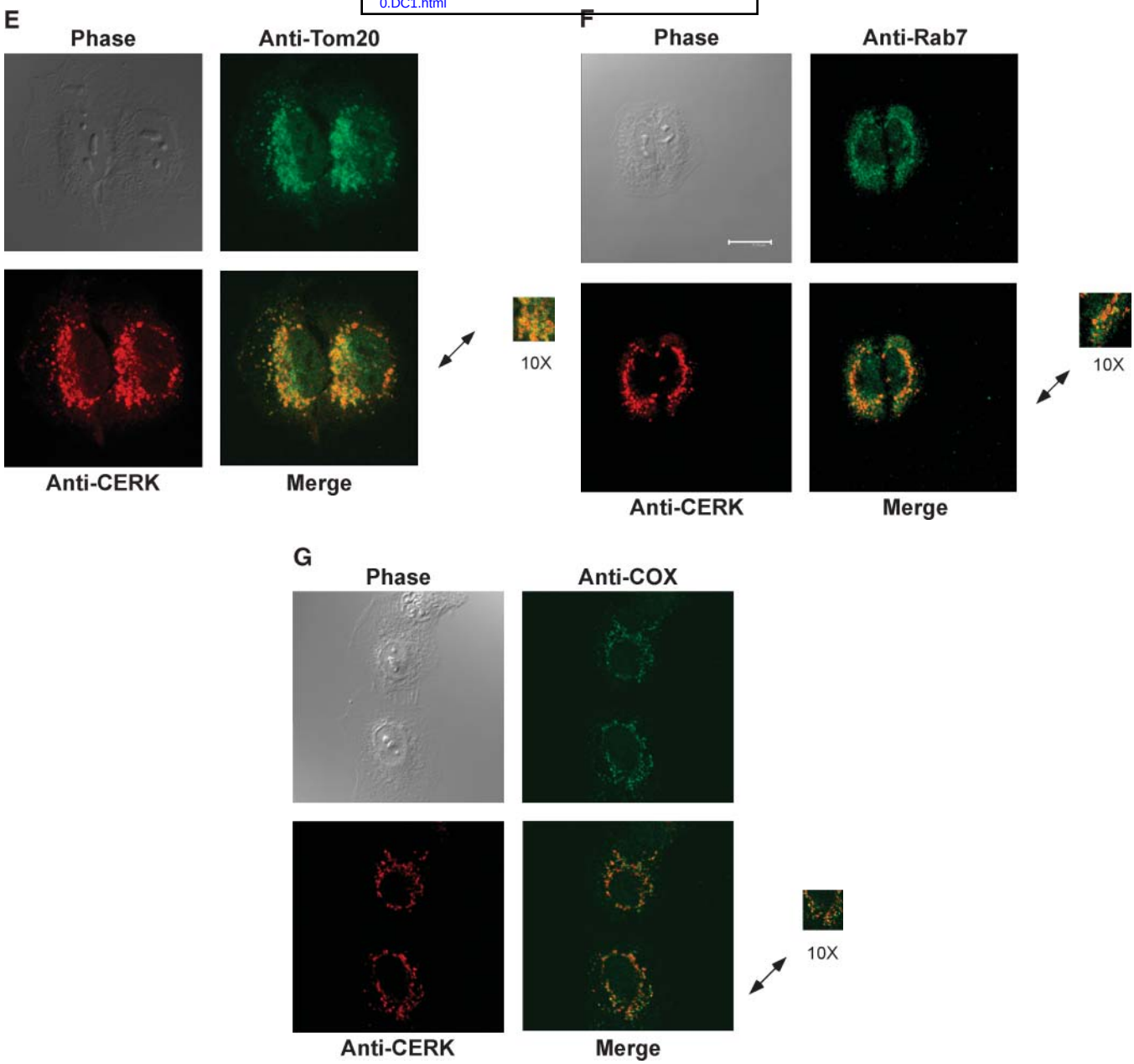

Fig. 5. *continued.*

the site of COX-2 localization in A549 cells (>70%) (38). The mitochondrial localization places CERK in the appropriate subcellular compartment for COX-2 and eicosanoid synthesis in A549 cells, which is confirmed in Fig. 5G.

Lastly, the localization of CERK was further confirmed by subcellular fractionation of the cells. **Figure 7** demonstrates that the heavy membrane fraction was enriched in mitochondria, *trans*-Golgi, and endosomal membranes. The light membrane fraction was enriched in *cis*-Golgi and endoplasmic reticulum membranes. CERK was detected only in the heavy membrane fraction, aiding confirmation of the confocal microscopy results. All of these data demonstrate that CERK localizes to internal membranes in cells, one of which is the *trans*-Golgi.

DISCUSSION

In this study, we show that the C1P subspecies profile was enriched in $C_{16:0}$ and $C_{18:0}$ C1P compared with ceramides, irrespective of agonist treatment. Furthermore, we show that CERK used ceramide transported in an active manner via CERT. Moreover, we demonstrate that CERK is localized to various perinuclear regions in A549 cells that are also sites of eicosanoid synthesis, specifically the TGN (**Fig. 8**). These findings are important for several reasons. First, we demonstrate where CERK is localized in cells by both biophysical and cell biological methods in accordance with eicosanoid synthesis. Second, substrate availability has now been shown to be a critical factor in regulating the formation of C1P in cells (basal and in-

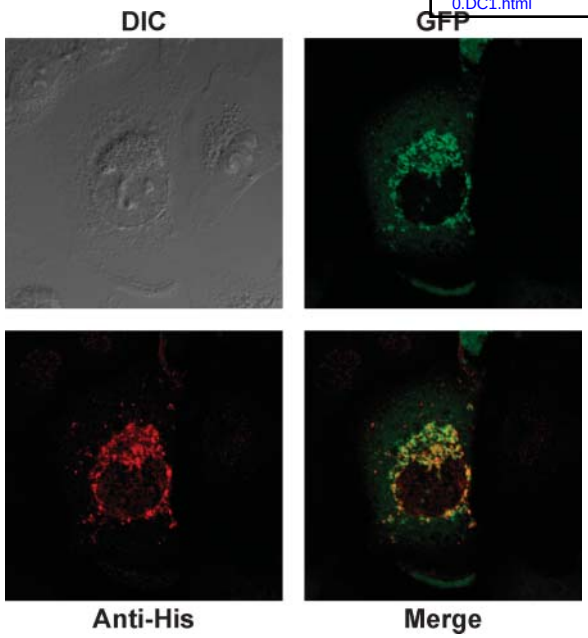

Fig. 6. CERK colocalizes with cytosolic phospholipase $A_2\alpha$ ($cPLA_2\alpha$) when activated with A23187. A549 cells were transfected as described in Experimental Procedures with adenovirus containing CERK and $cPLA_2$ for 48 h. Cells were treated for 10 min with 1 μM A23187 and fixed with 100% cold methanol. Cells were then incubated for 40 min with the primary antibody, a rabbit anti-6XHis (1:100) (Sigma) (red), as described in Experimental Procedures. Data are representative of two different experiments. DIC, differential interference contrast; GFP, green fluorescent protein.

duced). Lastly, CERT is now placed upstream of C1P generation, suggesting this factor as a possible therapeutic target for inflammatory conditions.

Previous studies from our laboratory demonstrated that C1P treatment induced the translocation of $cPLA_2\alpha$ to the Golgi apparatus. Furthermore, C1P was also shown to directly bind and activate $cPLA_2\alpha$, and siRNA specific to $cPLA_2\alpha$ blocked the ability of C1P to induce AA release (16). In this study, we have shown using CERT siRNA, SPR studies, subcellular fractionation, and confocal microscopy that CERK is located to the TGN and possibly to endosomal/exosomal compartments and the mitochondria. Thus, the enzyme that produces C1P is localized to the proper cell location for the interaction and activation of $cPLA_2\alpha$, supporting our reports that C1P is an endogenous activator of the enzyme in response to inflammatory agonists (9). In this regard, CERK and $cPLA_2\alpha$ showed colocalization of these two enzymes when activated by A23187. Furthermore, both $cPLA_2\alpha$ and COX-2 are responsible for the production of PGE_2 in response to IL-1β in A549 cells. Thus, the observation that CERK colocalizes with COX-2 places CERK in the proper subcellular localization for the regulation of this pathway. Therefore, these findings are in accord with our previous report demonstrating that siRNA against CERK is a potent inhibitor of PGE_2 synthesis in response to IL-1β.

The demonstration that CERK requires ceramide supplied by CERT is very indicative of a *trans*-Golgi localization, as CERT has been established to transport saturated ceramides (≤22 carbon acyl chain) to the TGN in an active manner (21, 35, 39). Importantly, the production of kinase-derived C1P in cells is more indicative of the use of CERT-supplied ceramide than sphingomyelin (SM) in the cells we examined in this study. Although the SM profile produced by mass spectrometry analysis demonstrates greatly reduced amounts of both dihydro-SM and $C_{24:0}$ SM compared with ceramide (see supplementary Fig. II), an enrichment of $C_{18:0}$ and $C_{20:0}$ (more indicative of CERT-transported ceramide) was not observed in contrast to C1P. On the surface, this finding seems to contrast with the reports by Hanada and coworkers (21), but it simply suggests that our cell types produce a majority of SM in the plasma membrane or that SM derived from serum in the medium affects the SM "pools" in the cells (40). Indeed, certain cell types that produce a majority of their SM in the plasma membrane would be exceptions to the Hanada hypothesis for SM synthesis in the context of CERT (35). Unpublished findings from our laboratory using RNA interference technology targeted to SM synthase 1 and 2 suggest that A549 cells produce a large portion of SM in a cellular compartment other than the *trans*-Golgi.

The requirement of CERT-supplied ceramide as a substrate for CERK in cells also explained the conundrum in the enrichment of specific C1P subspecies (e.g., $C_{18:0}$ C1P) in cells versus the knowledge that CERK does not demonstrate substrate preference for saturated versus unsaturated ceramide in vitro (34). These data also suggest that

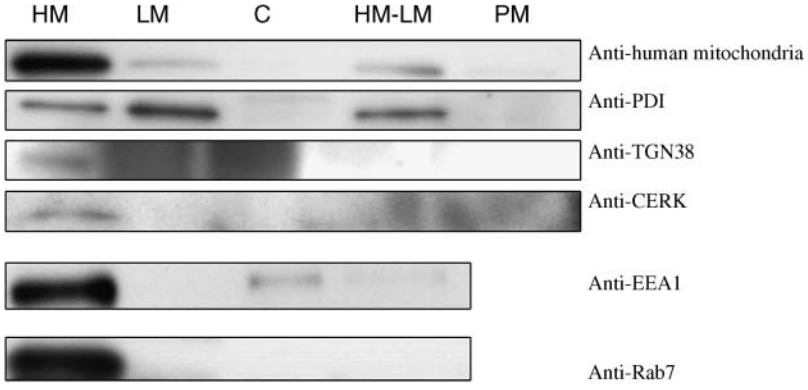

Fig. 7. CERK localizes to heavy membranes in A549 cells. A549 cells were fractionated into heavy membranes (HM), light membranes (LM), plasma membrane (PM), and cytosol (C), as detailed in Experimental Procedures. Samples were analyzed by Western blot using rabbit anti-human mitochondrial antibody (1:1,000) (US Biological), mouse anti-protein disulfide isomerase (PDI) antibody (1:1,000) (Stressgen), rabbit anti-TGN46 antibody (1:1,000) (Abcam), mouse anti-TGN38 antibody (1:1,000) (Affinity Bioreagents), mouse anti-CERK antibody (1:10), rabbit anti-EEA1 antibody (1:500) (Abcam), and rabbit anti-Rab7 antibody (1:500) (Sigma).

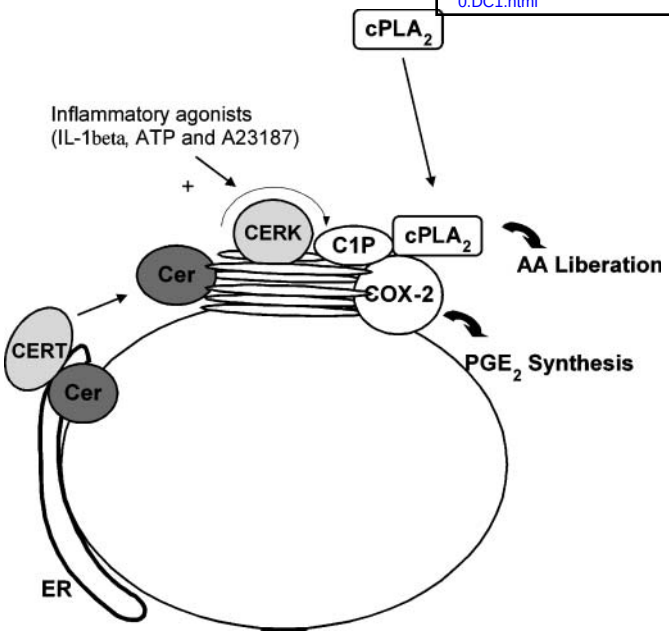

Fig. 8. Scheme of the intracellular signaling of the interplay between sphingolipid metabolism and eicosanoid biosynthesis. The figure depicts the hypothetical activation of CERK by inflammatory agonists [e.g., interleukin (IL)-1β] to produce C1P and activate the eicosanoid cascade. AA, arachidonic acid; Cer, ceramide; ER, endoplasmic reticulum; PGE_2, prostaglandin E_2.

substrate availability was one mechanism to regulate both the type and the amount of C1P produced. Interestingly, unpublished findings from our laboratory demonstrate that C1P treatment activates $cPLA_2\alpha$ and induces AA release irrespective of the acyl chain length. Thus, it is likely that the amount of C1P produced as well as cellular location, but not the type of C1P, are the critical factors in the induction of eicosanoid synthesis.

Previous reports from our laboratory showed that IL-1β is an activator of CERK (9). In this regard, the observation that downregulation of CERT dramatically affects the production of C1P and PGE_2 synthesis in response to IL-1β in the cells demonstrates that CERT is upstream of CERK and, thus, of $cPLA_2\alpha$. This was not attributable to an indirect effect on the Golgi apparatus, as CERT siRNA had no effect on *trans*-Golgi or *cis*-Golgi structure. These data raise the possibility that CERT may be an anti-inflammatory target by simply decreasing the amount of C1P in the cell (Fig. 8). These data do not support or refute the activation/enhancement of CERT-supplied ceramide in IL-1β-induced eicosanoid signaling, but coupled with our previous findings, they suggest the activation of CERK by a yet undisclosed mechanism. The activation of CERT is possible and an intriguing hypothesis to explore.

The *trans*-Golgi and possible endosomal localization of CERK may also suggest a role for this enzyme in vesicle trafficking/exocytosis. In this regard, a recent report by Igarashi and coworkers (11, 41) demonstrated that C1P induced the release of β-hexosaminidase from RBL-2H3 cells via CERK. The localization of CERK to the *trans*-Golgi apparatus is also in accordance with the report by Carre and coworkers (10), who reported that overexpression of CERK tagged with green fluorescent protein (not endogenous CERK) in COS-1 cells results in localization to perinuclear/Golgi membrane using a fluorescent ceramide as a Golgi marker. Both this laboratory group and Kim, Mitsutake, and Igarashi (42) also recently demonstrated that osmotic shock led to the trafficking of CERK-containing vesicles to the plasma membrane. Unpublished findings from our laboratory also found trafficking of CERK to the plasma membrane in response to long-term exposure to A23187. Our localization of CERK to late endosomes and exosomes using a Rab7 antibody further supports the hypothesis that CERK and C1P have roles in exocytosis, vesicle trafficking, and possibly phagocytosis/membrane fusion.

In conclusion, these studies demonstrate (by several different techniques) that CERK is localized to subcellular compartments important for eisosanoid synthesis in A549 cells, specifically the *trans*-Golgi apparatus. Furthermore, we demonstrate that CERK mainly uses ceramides transported to the *trans*-Golgi via CERT. Thus, the anabolic pathway for the production of basal as well as agonist-induced C1P is now defined. Lastly, we demonstrate that CERT is upstream of CERK and may be a possible target for the development of anti-inflammatory therapeutics.

This work was supported by grants from the Veterans Administration (VA Merit Review I to C.E.C.), Virginia Commonwealth University funds (to C.E.C.), the National Institutes of Health (Grant HL-072925 to C.E.C., Grant CA-117990 to C.E.C., Grant GM-52598 to W.C., and Grant 1C06 RR-17393 to Virginia Commonwealth University for laboratory renovation), the Lipid MAPS Consortium (Grant GM069338 to A.H.M.), and American Heart Association Postdoctoral Fellowship AHA0625502U (to N.F.L.). The CERT antibody was generously provided by Dr. J. Saus and F. Revert-Ros. The TOM-20 antibody was generously provided by Dr. B. Wattenberg. Microscopy was performed at the Virginia Commonwealth University Department of Neurobiology and Anatomy Microscopy Facility, supported, in part, by funding from National Institutes of Health-National Institute of Neurological Disorders and Stroke Center Core Grant 5P30 NS-047463. The authors thank Dr. Scott Henderson of the Anatomy Microscopy Facility for his technical advice. Lastly, the authors thank Exalpha for the CERK monoclonal antibody.

REFERENCES

1. Kolesnick, R. N., and M. R. Hemer. 1990. Characterization of a ceramide kinase activity from human leukemia (HL-60) cells. Separation from diacylglycerol kinase activity. *J. Biol. Chem.* **265:** 18803–18808.
2. Dressler, K. A., and R. N. Kolesnick. 1990. Ceramide 1-phosphate, a novel phospholipid in human leukemia (HL-60) cells. Synthesis via ceramide from sphingomyelin. *J. Biol. Chem.* **265:** 14917–14921.
3. Bajjalieh, S. M., T. F. Martin, and E. Floor. 1989. Synaptic vesicle ceramide kinase. A calcium-stimulated lipid kinase that co-purifies with brain synaptic vesicles. *J. Biol. Chem.* **264:** 14354–14360.
4. Bajjalieh, S., and R. Batchelor. 2000. Ceramide kinase. *Methods Enzymol.* **311:** 207–215.
5. Sugiura, M., K. Kono, H. Liu, T. Shimizugawa, H. Minekura, S. Spiegel, and T. Kohama. 2002. Ceramide kinase, a novel lipid

kinase. Molecular cloning and functional characterization. *J. Biol. Chem.* **277:** 23294–23300.
6. Hinkovska-Galcheva, V. T., L. A. Boxer, P. J. Mansfield, D. Harsh, A. Blackwood, and J. A. Shayman. 1998. The formation of ceramide-1-phosphate during neutrophil phagocytosis and its role in liposome fusion. *J. Biol. Chem.* **273:** 33203–33209.
7. Rile, G., Y. Yatomi, T. Takafuta, and Y. Ozaki. 2003. Ceramide 1-phosphate formation in neutrophils. *Acta Haematol.* **109:** 76–83.
8. Riboni, L., R. Bassi, V. Anelli, and P. Viani. 2002. Metabolic formation of ceramide-1-phosphate in cerebellar granule cells: evidence for the phosphorylation of ceramide by different metabolic pathways. *Neurochem. Res.* **27:** 711–716.
9. Pettus, B. J., A. Bielawska, S. Spiegel, P. Roddy, Y. A. Hannun, and C. E. Chalfant. 2003. Ceramide kinase mediates cytokine- and calcium ionophore-induced arachidonic acid release. *J. Biol. Chem.* **278:** 38206–38213.
10. Carre, A., C. Graf, S. Stora, D. Mechtcheriakova, R. Csonga, N. Urtz, A. Billich, T. Baumruker, and F. Bornancin. 2004. Ceramide kinase targeting and activity determined by its N-terminal pleckstrin homology domain. *Biochem. Biophys. Res. Commun.* **324:** 1215–1219.
11. Mitsutake, S., T. J. Kim, Y. Inagaki, M. Kato, T. Yamashita, and Y. Igarashi. 2004. Ceramide kinase is a mediator of calcium-dependent degranulation in mast cells. *J. Biol. Chem.* **279:** 17570–17577.
12. Gomez-Munoz, A., P. A. Duffy, A. Martin, L. O'Brien, H. S. Byun, R. Bittman, and D. N. Brindley. 1995. Short-chain ceramide-1-phosphates are novel stimulators of DNA synthesis and cell division: antagonism by cell-permeable ceramides. *Mol. Pharmacol.* **47:** 833–839.
13. Gomez-Munoz, A., J. Y. Kong, B. Salh, and U. P. Steinbrecher. 2004. Ceramide-1-phosphate blocks apoptosis through inhibition of acid sphingomyelinase in macrophages. *J. Lipid Res.* **45:** 99–105.
14. Hinkovska-Galcheva, V., L. A. Boxer, A. Kindzelskii, M. Hiraoka, A. Abe, S. Goparju, S. Spiegel, H. R. Petty, and J. A. Shayman. 2005. Ceramide 1-phosphate, a mediator of phagocytosis. *J. Biol. Chem.* **280:** 26612–26621.
15. Mitsutake, S., and Y. Igarashi. 2005. Calmodulin is involved in the Ca^{2+}-dependent activation of ceramide kinase as a calcium sensor. *J. Biol. Chem.* **280:** 40436–40441.
16. Pettus, B. J., A. Bielawska, P. Subramanian, D. S. Wijesinghe, M. Maceyka, C. C. Leslie, J. H. Evans, J. Freiberg, P. Roddy, Y. A. Hannun, et al. 2004. Ceramide 1-phosphate is a direct activator of cytosolic phospholipase A2. *J. Biol. Chem.* **279:** 11320–11326.
17. Grewal, S., S. Ponnambalam, and J. H. Walker. 2003. Association of cPLA2-alpha and COX-1 with the Golgi apparatus of A549 human lung epithelial cells. *J. Cell Sci.* **116:** 2303–2310.
18. Lassus, P., X. Opitz-Araya, and Y. Lazebnik. 2002. Requirement for caspase-2 in stress-induced apoptosis before mitochondrial permeabilization. *Science.* **297:** 1352–1354.
19. Laemmli, U. K. 1970. Cleavage of structural proteins during the assembly of the head of bacteriophage T4. *Nature.* **227:** 680–685.
20. Towbin, H., T. Staehelin, and J. Gordon. 1979. Electrophoretic transfer of proteins from polyacrylamide gels to nitrocellulose sheets: procedure and some applications. *Proc. Natl. Acad. Sci. USA.* **76:** 4350–4354.
21. Hanada, K., K. Kumagai, S. Yasuda, Y. Miura, M. Kawano, M. Fukasawa, and M. Nishijima. 2003. Molecular machinery for non-vesicular trafficking of ceramide. *Nature.* **426:** 803–809.
22. Raya, A., F. Revert-Ros, P. Martinez-Martinez, S. Navarro, E. Rosello, B. Vieites, F. Granero, J. Forteza, and J. Saus. 2000. Goodpasture antigen-binding protein, the kinase that phosphorylates the goodpasture antigen, is an alternatively spliced variant implicated in autoimmune pathogenesis. *J. Biol. Chem.* **275:** 40392–40399.
23. Bligh, E. G., and W. J. Dyer. 1959. A rapid method of total lipid extraction and purification. *Can. J. Biochem. Physiol.* **37:** 911–917.
24. Perry, D. K., A. Bielawska, and Y. A. Hannun. 2000. Quantitative determination of ceramide using diglyceride kinase. *Methods Enzymol.* **312:** 22–31.
25. Sullards, M. C., and A. H. Merrill, Jr. 2001. Analysis of sphingosine 1-phosphate, ceramides, and other bioactive sphingolipids by high-performance liquid chromatography-tandem mass spectrometry. *Sci. STKE.* **2001:** PL1.
26. Merrill, A. H., Jr., M. C. Sullards, J. C. Allegood, S. Kelly, and E. Wang. 2005. Sphingolipidomics: high-throughput, structure-specific, and quantitative analysis of sphingolipids by liquid chromatography tandem mass spectrometry. *Methods.* **36:** 207–224.
27. Stahelin, R. V., J. D. Rafter, S. Das, and W. Cho. 2003. The molecular basis of differential subcellular localization of C2 domains of protein kinase C-alpha and group IVa cytosolic phospholipase A2. *J. Biol. Chem.* **278:** 12452–12460.
28. Stahelin, R. V., B. Ananthanarayanan, N. R. Blatner, S. Singh, K. S. Bruzik, D. Murray, and W. Cho. 2004. Mechanism of membrane binding of the phospholipase D1 PX domain. *J. Biol. Chem.* **279:** 54918–54926.
29. Bittova, L., R. V. Stahelin, and W. Cho. 2001. Roles of ionic residues of the C1 domain in protein kinase C-alpha activation and the origin of phosphatidylserine specificity. *J. Biol. Chem.* **276:** 4218–4226.
30. Stahelin, R. V., and W. Cho. 2001. Differential roles of ionic, aliphatic, and aromatic residues in membrane-protein interactions: a surface plasmon resonance study on phospholipases A2. *Biochemistry.* **40:** 4672–4678.
31. Stahelin, R. V., F. Long, K. Diraviyam, K. S. Bruzik, D. Murray, and W. Cho. 2002. Phosphatidylinositol 3-phosphate induces the membrane penetration of the FYVE domains of Vps27p and Hrs. *J. Biol. Chem.* **277:** 26379–26388.
32. Manders, E., F. J. Verbeek, and A. J. Aten. 1993. Measurement of co-localization of objects in dualcolor confocal images. *J. Microsc.* **169:** 375–382.
33. Maceyka, M., V. E. Nava, S. Milstien, and S. Spiegel. 2004. Aminoacylase 1 is a sphingosine kinase 1-interacting protein. *FEBS Lett.* **568:** 30–34.
34. Wijesinghe, D. S., A. Massiello, P. Subramanian, Z. Szulc, A. Bielawska, and C. E. Chalfant. 2005. Substrate specificity of human ceramide kinase. *J. Lipid Res.* **46:** 2706–2716.
35. Kumagai, K., S. Yasuda, K. Okemoto, M. Nishijima, S. Kobayashi, and K. Hanada. 2005. CERT mediates intermembrane transfer of various molecular species of ceramides. *J. Biol. Chem.* **280:** 6488–6495.
36. McMurray, W. C., and L. Rogers. 1973. Phospholipid and protein metabolism in mouse liver mitochondria during riboflavin deficiency and recovery. *Can. J. Biochem.* **51:** 1262–1274.
37. Wisner, T. W., and D. C. Johnson. 2004. Redistribution of cellular and herpes simplex virus proteins from the trans-Golgi network to cell junctions without enveloped capsids. *J. Virol.* **78:** 11519–11535.
38. Liou, J. Y., N. Aleksic, S. F. Chen, T. J. Han, S. K. Shyue, and K. K. Wu. 2005. Mitochondrial localization of cyclooxygenase-2 and calcium-independent phospholipase A2 in human cancer cells: implication in apoptosis resistance. *Exp. Cell Res.* **306:** 75–84.
39. Perry, R. J., and N. D. Ridgway. 2005. Molecular mechanisms and regulation of ceramide transport. *Biochim. Biophys. Acta.* **1734:** 220–234.
40. Koval, M., and R. E. Pagano. 1991. Intracellular transport and metabolism of sphingomyelin. *Biochim. Biophys. Acta.* **1082:** 113–125.
41. Kim, J. W., Y. Inagaki, S. Mitsutake, N. Maezawa, S. Katsumura, Y. W. Ryu, C. S. Park, M. Taniguchi, and Y. Igarashi. 2005. Suppression of mast cell degranulation by a novel ceramide kinase inhibitor, the F-12509A olefin isomer K1. *Biochim. Biophys. Acta.* **1738:** 82–90.
42. Kim, T. J., S. Mitsutake, and Y. Igarashi. 2006. The interaction between the pleckstrin homology domain of ceramide kinase and phosphatidylinositol 4,5-bisphosphate regulates the plasma membrane targeting and ceramide 1-phosphate levels. *Biochem. Biophys. Res. Commun.* **342:** 611–617.